Carcinoembryonic Antigen-Related Cell Adhesion Molecule 1

A Link Between Insulin and Lipid Metabolism

Anthony M. DeAngelis,[1] Garrett Heinrich,[1] Tong Dai,[1] Thomas A. Bowman,[1] Payal R. Patel,[1] Sang Jun Lee,[1] Eun-Gyoung Hong,[2] Dae Young Jung,[2] Anke Assmann,[3] Rohit N. Kulkarni,[3] Jason K. Kim,[2] and Sonia M. Najjar[1]

OBJECTIVE—Liver-specific inactivation of carcinoembryonic antigen-related cell adhesion molecule 1 (CEACAM1) by a dominant-negative transgene (L-SACC1 mice) impaired insulin clearance, caused insulin resistance, and increased hepatic lipogenesis. To discern whether this phenotype reflects a physiological function of CEACAM1 rather than the effect of the dominant-negative transgene, we characterized the metabolic phenotype of mice with null mutation of the Ceacam1 gene ($Cc1^{-/-}$).

RESEARCH DESIGN AND METHODS—Mice were originally generated on a mixed C57BL/6x129sv genetic background and then backcrossed 12 times onto the C57BL/6 background. More than 70 male mice of each of the $Cc1^{-/-}$ and wild-type $Cc1^{+/+}$ groups were subjected to metabolic analyses, including insulin tolerance, hyperinsulinemic-euglycemic clamp studies, insulin secretion in response to glucose, and determination of fasting serum insulin, C-peptide, triglyceride, and free fatty acid levels.

RESULTS—Like L-SACC1, $Cc1^{-/-}$ mice exhibited impairment of insulin clearance and hyperinsulinemia, which caused insulin resistance beginning at 2 months of age, when the mutation was maintained on a mixed C57BL/6x129sv background, but not until 5–6 months of age on a homogeneous inbred C57BL/6 genetic background. Hyperinsulinemic-euglycemic clamp studies revealed that the inbred $Cc1^{-/-}$ mice developed insulin resistance primarily in liver. Despite substantial expression of CEACAM1 in pancreatic β-cells, insulin secretion in response to glucose in vivo and in isolated islets was normal in $Cc1^{-/-}$ mice (inbred and outbred strains).

CONCLUSIONS—Intact insulin secretion in response to glucose and impairment of insulin clearance in L-SACC1 and $Cc1^{-/-}$ mice suggest that the principal role of CEACAM1 in insulin action is to mediate insulin clearance in liver. ***Diabetes*** **57: 2296–2303, 2008**

From the [1]Center for Diabetes and Endocrine Research and the Department of Physiology and Pharmacology, University of Toledo College of Medicine, Toledo, Ohio; the [2]Department of Cellular and Molecular Physiology, Pennsylvania State University College of Medicine, Hershey, Pennsylvania; and the [3]Research Division, Joslin Diabetes Center, Boston, Massachusetts.
Corresponding author: Sonia M. Najjar, sonia.najjar@utoledo.edu.
Received 17 March 2008 and accepted 2 June 2008.
Published ahead of print at http://diabetes.diabetesjournals.org on 10 June 2008. DOI: 10.2337/db08-0379.
A.M.D. and G.H. contributed equally to this work. T.A.B. and P.R.P. contributed equally to this work.

In response to physiological stimuli, insulin is secreted from pancreatic β-cells into the portal circulation in a pulsatile manner. Through its first passage, ~50% of the secreted insulin is cleared in liver. Insulin clearance is a critical regulator of insulin action. Impaired insulin clearance is seen in response to peripheral insulin resistance. On the other hand, impaired insulin clearance can be the primary cause of insulin resistance by causing downregulation of insulin receptors and hepatic lipogenesis, both of which result in insulin resistance (1–3).

Insulin clearance in liver is mediated by receptor-mediated insulin endocytosis followed by degradation (1,4). Upon its phosphorylation by the insulin receptor, the carcinoembryonic antigen-related cell adhesion molecule 1 (CEACAM1) takes part of the insulin-receptor endocytosis complex to promote insulin uptake and removal in the hepatocyte (5–7). Moreover, liver-specific overexpression of a dominant-negative S503A phosphorylation-defective isoform of CEACAM1 impairs insulin clearance and causes chronic hyperinsulinemia and insulin resistance, together with increased visceral obesity and dyslipidemia in L-SACC1 mice (8–10). In agreement with this finding, activation of SHP-1, a CEACAM1 phosphatase, adversely affects glucose homeostasis by impairing insulin clearance (9). These data suggest that CEACAM1 regulates insulin action by promoting hepatic insulin clearance.

To further investigate its function in insulin action in vivo, we have characterized the metabolic phenotype of the $Cc1^{-/-}$ mice homozygous for null mutation of the Ceacam1 gene. We report here that, similar to liver-specific inactivation of CEACAM1, its null mutation causes impaired insulin clearance, hyperinsulinemia, hepatic steatosis, and visceral adiposity. Moreover, the phenotype is associated with hepatic insulin resistance, which is evident at an earlier age, when the mutation is propagated on a mixed C57BL/6x129sv compared with a homogenous C57BL/6 genetic background. These data suggest that the principal role of CEACAM1 is to promote insulin clearance in liver.

RESEARCH DESIGN AND METHODS

Animal husbandry. $Cc1^{-/-}$-null mice were generated on a mixed C57BL/6x129sv background and backcrossed 12 times onto the C57BL/6 background (11). Animals were kept in a 12-h dark/light cycle and fed standard chow ad libitum. All procedures were approved by the Institutional Animal Care and Utilization Committee. Male mice from 2 to 10 months of age were studied.

TABLE 1
Metabolic parameters of inbred C57BL/6 mice

	2 months		6 months	
	Cc1$^{+/+}$	*Cc1*$^{-/-}$	*Cc1*$^{+/+}$	*Cc1*$^{-/-}$
Body wt (g)	21. ± 0.2	22. ± 0.3*	27. ± 0.3	31. ± 0.3*
Visceral fat/body wt (%)	0.9 ± 0.1	1.2 ± 0.1*	1.9 ± 0.1*	3.3 ± 0.3*
Lean mass/body wt (%)	85. ± 0.7	84. ± 0.7	78. ± 0.9	73. ± 1.2*
Total fat/body wt (%)	15. ± 0.7	16. ± 0.7	22. ± 0.9	27. ± 1.2*
Serum insulin (ng/ml)	0.6 ± 0.0	0.8 ± 0.1*	0.4 ± 0.0	0.8 ± 0.1*
Serum C-peptide (ng/ml)	1.7 ± 0.3	2.4 ± 0.2*	0.6 ± 0.1	1.2 ± 0.3*
Steady-state C/I	5.0 ± 0.5	3.9 ± 0.2*	3.1 ± 0.2	2.4 ± 0.2*
Serum FFA (mEq/l)	0.5 ± 0.0	0.5 ± 0.0	0.7 ± 0.1	1.0 ± 0.1*
Serum triglyceride (mg/dl)	51. ± 3.2	62. ± 2.5*	61. ± 5.0	54. ± 2.4
Fasting glucose (mg/dl)	123. ± 2.0	112. ± 1.9*	102. ± 1.8	96 ± 2.1*
Random glucose (mg/dl)	137. ± 14.0	119. ± 2.11	119. ± 2.12	100. ± 3.29*
Hepatic triglyceride (μg/mg protein)	89.0 ± 7.10	133. ± 13.6*	62.7 ± 8.3	97.7 ± 9.43*
Muscle triglyceride (μg/mg protein)	11.4 ± 1.90	8.20 ± 2.10	4.36 ± 0.75	6.39 ± 1.62

Data are means ± SE. *$P < 0.05$ *Cc1*$^{-/-}$ vs. *Cc1*$^{+/+}$ control mice.

Metabolic analysis. After an overnight fast (from 1700 until 1100 h the next day), mice were anesthetized with sodium pentobarbital (55 mg/kg body wt), and whole venous blood was drawn from retroorbital sinuses to measure fasting glucose levels using a glucometer (Accu-chek Aviva; Roche), serum insulin and C-peptide levels by radioimmunoassays (Linco), serum FFAs by NEFA C kit (Wako), and serum triglycerides (Pointe Scientific). Serum total bilirubin and cholesterol were measured using a bilirubin calibrator and Infinity Cholesterol reagent (Sigma), respectively, and blood uric acid was measured using Infinity BUN reagent (Sigma). Visceral adiposity was expressed as percentage weight of white adipose tissue per total body weight.

Hyperinsulinemic-euglycemic clamps to assess insulin action in vivo. After an overnight fast, a 2-h hyperinsulinemic-euglycemic clamp was conducted in awake mice (n = 11~12) with a primed (150 mU/kg body wt) and continuous infusion of human regular insulin (Humulin) at a rate of 2.5 mU · kg^{-1} · min^{-1} to raise serum insulin within a physiological range (10). Basal and insulin-stimulated whole-body glucose turnover were estimated with a continuous infusion of [3-^{3}H]glucose (PerkinElmer Life and Analytical Sciences) for 2 h before (0.05 μCi/min) and throughout the clamps (0.1 μCi/min). Tissues were removed to determine glycogen (10) and triglyceride (12) content.

Insulin tolerance test. After an overnight fast (1700 until 1100 h the next day), mice were anesthetized and injected intraperitoneally with 0.125 units insulin/kg body wt, and their venous blood from the retroorbital sinuses was drawn at 0–5 h after injection to determine blood glucose levels.

Intraperitoneal glucose tolerance test and acute insulin secretion. After an overnight fast (1700 until 0800 h the next day), anesthetized mice were injected intraperitoneally with glucose (2.0 g/kg body wt), and their venous blood was drawn at 0–30 min after injection to determine blood glucose and serum insulin levels.

Glucose-6-phosphate content. Liver was removed from randomly fed mice and snap-frozen, and glucose-6-phosphate (G6P) content was determined in 1-g tissue homogenates using G6P dehydrogenase (12). Absorbance was measured at 340 nm before and after addition of enzyme.

Cell culture. Murine α-TC6 cells (13) and Min-6 β-cells (14) were maintained at 37°C and 5% CO_2 in Dulbecco's modified Eagle's medium containing 10% fetal bovine serum and penicillin and streptomycin. All experiments were performed on 80% confluent cells.

Western blot. The concentration of proteins in tissue and serum lysates was quantitated by BCA protein assay (Pierce) before analysis by 7 or 4–12% gradient SDS-PAGE (Invitrogen), respectively, and immunoprobing with specific antibodies. These included polyclonal antibodies against ApoB48/100 (Chemicon International), fatty acid synthase (FAS) (15), and fatty acid transporter-1 (FATP-1) (I-20; Santa Cruz Biotechnology) in addition to monoclonal antibodies against actin (Sigma) and tubulin (Sigma). Blots were incubated with horseradish peroxidase–conjugated anti-goat IgG (Santa Cruz Biotechnology), anti-mouse IgG (Amersham), and anti-rabbit IgG (Amersham) antibodies, and proteins were detected by enhanced chemiluminescence (Amersham) and quantified by densitometry.

Pancreatic cells were lysed, and 1 mg protein was subjected to immunoprecipitation, as previously described with an anti-mouse polyclonal antibody against BGP1 (α-mCC1; Ab-231) (16) and analysis on SDS-PAGE, followed by immunoprobing with Ab-231 to normalize for the amount of CEACAM1 in the immunopellet.

For phosphorylation experiments, livers were removed, and 200 μg lysates was treated with 100 nmol/l insulin for 5 min before immunoprecipitation with antibodies against the β-subunit of the insulin receptor (α-IR$_\beta$) (Santa Cruz Biotechnology) followed by SDS-PAGE analysis and immunoblotting with α-phosphotyrosine antibody (α-pTyr) (Upstate Biotechnology), followed by α-IR$_\beta$ to normalize against the amount of insulin receptor in the immunopellet.

Northern blot. Liver mRNA was purified using TRIzol (Invitrogen) followed by the MicroPoly (A) Pure kit (Ambion) and analysis by probing with cDNAs for glucose-6-phosphatase (G6Pase), carnitine palmitoyl transferase 1 (CPT1), PEPCK, pyruvate dehydrogenate kinase (PDK-4), glucokinase, and sterol regulatory element–binding protein 1c (SREBP-1c), using the Random Primed DNA Labeling kit (Roche) before reprobing with β-actin cDNA to normalize against the amount of mRNA applied.

Insulin secretion from isolated islets. Islets were purified from pancreata of 6-month-old mice by collagenase digestion (17). Islets were resuspended in RPMI containing 10% newborn calf serum and 5.5 mmol/l glucose and cultured overnight at 37°C. Islets were stimulated with glucose (2.8–16.8 mmol/l) or 20 mmol/l KCl for 1 h at 37°C and collected by centrifugation, and the supernatant was assayed for insulin content by radioimmunoassay. Islets were dissolved in high-salt buffer and sonicated three times at 80 watts for 10 s, and DNA concentration was determined to normalize insulin content.

Fluorescence-activated cell sorter purification of isolated islets. Islets were isolated by the intraductal collagenase digestion method (18). After PBS wash, the suspension was passed through a 35-μm filter before fluorescence-activated cell sorter (FACS) analysis, based on autofluorescence and size (19). Cells were sorted directly into TRIzol reagent, and the purity of the sorted fractions was determined by real-time PCR for insulin and glucagon in each fraction.

β-Cell area and immunohistochemistry. Mice were anesthetized, and pancreata were dissected, weighed, fixed in Bouin's solution, sectioned, and stained (20). Antibodies used for the immunofluorescence staining were: guinea pig anti-human insulin (Linco Research) and AMCA-conjugated donkey anti–guinea pig antibody (Jackson Immunoresearch) for insulin; anti-mouse glucagons monoclonal antibody (Sigma) and Texas red–conjugated donkey anti-mouse antibody (Jackson Immunoresearch) for glucagon; and anti-somatostatin rabbit polyclonal antibody (Abcam) and Cy2-conjugated donkey anti-rabbit antibody (Jackson Immunoresearch) for somatostatin. β-Cell area was calculated by morphometric analysis using Image J software (National Institutes of Health; http://rsb.info.nih.gov/ij/), and the insulin-stained area was divided by total pancreas area.

Real-time PCR. RNA was extracted using TRIzol method according to the manufacturer's protocol. After DNAse digestion (DNAfree; Ambion), 100 ng RNA was transcribed into cDNA in a 20-μl reaction using a High Capacity cDNA Archive kit (Applied Biosystems), analyzed, and amplified (ABI 7900 HT system). PCR was performed in a 10-μl reaction, containing 5 μl cDNA (one-fifth diluted), 1×SYBR Green PCR Master Mix (Applied Biosystems), and 300 nmol/l of each primer: Ceacam1 forward primer, AATCTGCCCCTGG CGCTTGGAGCC; Ceacam1 reverse primer, AAATCGCACAGTCGCCTGAG TACG; β-actin forward primer, AGGGCTATGCTCTCCCTCAC; and β-actin reverse primer, AAGGAAGGCTGGAAAAGAGC.

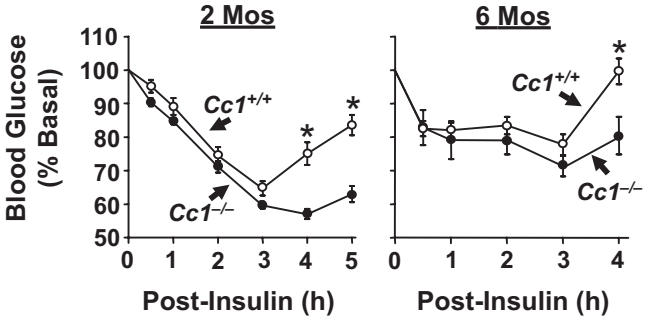

FIG. 1. Insulin tolerance test in inbred mice. Glucose levels were measured in venous blood extracted from overnight-fasted 2- and 6-month-old age-matched wild-type ($Cc1^{+/+}$, ○) and *Cc1* knockout mice ($Cc1^{-/-}$, ●) following an intraperitoneal injection with insulin (0.125 unit/kg) for 0–5 h. Experiments were performed on $n \geq 10$ per group. Values expressed as means ± SE. *$P < 0.05$ vs. $Cc1^{+/+}$.

Cycle threshold (Ct) values were used to calculate the amount of amplified PCR product relative to β-actin. The relative amount of mRNA was calculated as $2-\Delta CT$. Results are expressed in fold change as means ± SE.

Statistical analysis. Data were analyzed with SPSS software using one-factor ANOVA analysis or Student's *t* test. $P < 0.05$ was statistically significant.

RESULTS

Body weight and composition in inbred $Cc1^{-/-}$ mice. $Cc1^{-/-}$ mice on inbred C57BL/6 genetic background exhibit an increase in body weight in comparison with their wild-type ($Cc1^{+/+}$) counterparts, starting at 2 months of age (Table 1). Parallel increase in whole-body fat mass, as assessed by ^{1}H-magnetic resonance spectrometry (Table 1), is attributed to increased visceral adiposity, as measured by % visceral fat per body weight, but not to lean mass (Table 1).

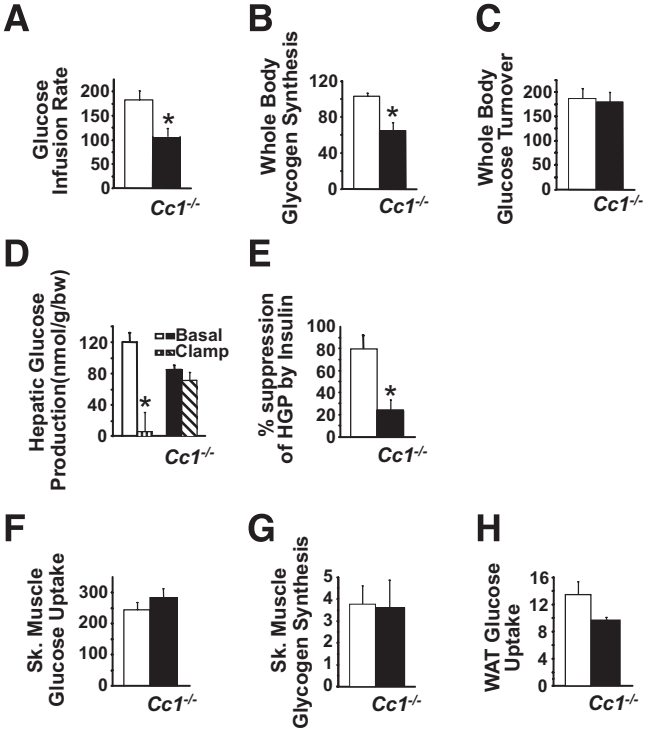

FIG. 2. Insulin response during hyperinsulinemic-euglycemic clamps in awake inbred mice. Five- to 6-month-old wild-type $Cc1^{+/+}$ (□) and $Cc1^{-/-}$ mice (■) ($n \geq 10$ per group) were subjected to clamp analysis. *A*: Steady-state glucose infusion rates during euglycemic clamps. *B*: Insulin-stimulated whole-body glycogen synthesis. *C*: Insulin-stimulated whole-body glucose turnover. *D*: HGP during basal and insulin-stimulated (clamp) states. *E*: Hepatic insulin action represented as insulin-mediated percent suppression of HGP. *F*: Insulin-stimulated glucose uptake in skeletal muscle (gastrocnemius). *G*: Skeletal muscle glycogen synthesis. *H*: Insulin-stimulated glucose uptake in white adipose tissue (WAT). Values (all in nmol · g^{-1} · min^{-1}) are expressed as means ± SE. *$P < 0.05$ vs. $Cc1^{+/+}$.

Hyperinsulinemia and impaired insulin clearance in inbred $Cc1^{-/-}$ mice. Null mutation of Ceacam1 does not alter liver function, as indicated by normal serum cholesterol (77.5 ± 5.30 in $Cc1^{-/-}$ vs. 86.0 ± 3.74 mg/dl in $Cc1^{+/+}$ mice; $P > 0.05$) and total bilirubin levels (0.29 ± 0.02 in $Cc1^{-/-}$ vs. 0.27 ± 0.02 mg/dl in $Cc1^{+/+}$ mice; $P > 0.05$). Similarly, kidney function, as assessed by normal serum uric acid level (1.38 ± 0.15 vs. 1.24 ± 0.11 mg/dl in $Cc1^{+/+}$ mice; $P > 0.05$), is intact in $Cc1^{-/-}$ mice.

Inbred $Cc1^{-/-}$ mice exhibit a slight increase (~1.5- to 2.0-fold) in fasting serum insulin levels, starting at 2 months of age (Table 1). Insulin clearance, measured by steady-state C-peptide–to–insulin molar ratio, is significantly reduced (by ~1.5-fold) in 2- to 6-month-old $Cc1^{-/-}$ relative to $Cc1^{+/+}$ mice (Table 1). Furthermore, insulin injection in 2- and 6-month-old $Cc1^{-/-}$ mice results in a prolonged suppression of blood glucose, as opposed to $Cc1^{+/+}$, in which glucose levels return to basal in 3–4 h (Fig. 1). This suggests that $Cc1^{-/-}$ mice clear exogenous insulin less efficiently. Taken together, the data propose that null mutation of Ceacam1 causes hyperinsulinemia and impairs insulin clearance.

Secondary insulin resistance in older inbred $Cc1^{-/-}$ mice. The steady-state glucose infusion rate required to maintain euglycemia during the clamp is normal in 3-month-old $Cc1^{-/-}$ mice (47.2 ± 1.8 vs. 48.0 ± 1.5 mg · kg^{-1} · min^{-1} in $Cc1^{+/+}$ mice; $P > 0.05$), suggesting intact insulin action at this age. Consistently, the suppressive effect of insulin on hepatic glucose production (HGP) is intact (97.3 ± 1.7 vs. 97.4 ± 1.3% in $Cc1^{+/+}$ mice; $P > 0.05$), and insulin-stimulated glucose uptake in white adipose tissue is elevated by ~twofold in these mice (28.0 ± 4.0 vs. 14.0 ± 3.0 nmol · g^{-1} · min^{-1} in $Cc1^{+/+}$ mice; $P < 0.05$).

In contrast, 6-month-old $Cc1^{-/-}$ mice exhibit reduction in steady-state glucose infusion rate (Fig. 2*A*), suggesting insulin resistance (Table 2). At this age, $Cc1^{-/-}$ mice exhibit a marked hepatic insulin resistance, as reflected by an ~14-fold increase in HGP during clamps (Fig. 2*D*) and reduced ability to suppress HGP (23.4 ± 10.2 vs. 79.6 ± 12.6% in $Cc1^{+/+}$ mice; $P < 0.005$) (Fig. 2*E*).

Insulin suppresses HGP by inhibiting gluconeogenesis and stimulating net hepatic glucose uptake and subsequent glycogen synthesis (21). Increase in fasting *Pepck* mRNA levels (Fig. 3*A*, i) suggests increased gluconeogenesis, and elevation in postprandial *Pdk4* with normal, rather than reduced, *Pepck* mRNA levels (Fig. 3*A*, ii) suggests that the suppressive effect of insulin on gluconeogenesis is reduced in older $Cc1^{-/-}$ mice. Together with increased fatty acid oxidation at the fed state, as suggested by higher *Cpt1* mRNA levels, and given that FFAs play a significant role in hepatic autoregulation of glucose production (22), the data suggest that the liver of $Cc1^{-/-}$ mice is geared toward gluconeogenesis, as manifested by higher levels of fed G6P content (0.31 ± 0.03 vs. 0.17 ± 0.05 μmol/g wet tissue in $Cc1^{+/+}$ mice; $P < 0.05$) (Fig. 3*B*) rather than glucose, due to reduced *G6Pase* mRNA levels (Fig. 3*A*, ii). This could in part underlie the lower basal HGP in the $Cc1^{-/-}$ mouse (84.6 ± 4.2 vs. 119.3 ± 12.1 nmol · g^{-1} · min^{-1} in $Cc1^{+/+}$ mice; $P < 0.05$).

Whole-body glycogen synthesis is decreased in adult $Cc1^{-/-}$ mice (Fig. 2*B*). With glycogen synthesis in muscle being normal ($P > 0.05$) (Fig. 2*G*), this suggests that the

TABLE 2
Metabolic parameters at basal state (overnight fasted) and during a 2-h hyperinsulinemic-euglycemic clamp experiment in 6-month-old inbred mice

			Basal period		Ccl clamp period	
	n	Body wt (g)	Plasma glucose (mmol/l)	Plasma insulin (μg/ml)	Plasma glucose (mmol/l)	Plasma insulin (μg/ml)
$Cc1^{+/+}$	5	23 ± 1	9.7 ± 0.4	0.08 ± 0.01	7.3 ± 0.5	0.51 ± 0.06
$Cc1^{-/-}$	7	29 ± 1*	8.5 ± 0.5	0.14 ± 0.02*	6.9 ± 0.4	0.60 ± 0.08

Data are means ± SE. *$P < 0.05$ vs. $Cc1^{+/+}$ mice by Student's t test.

decrease in glycogen synthesis is primarily hepatic. With the mRNA level of fed hepatic *glucokinase* being intact (Fig. 3*A*, ii), it is possible that the increase in G6P content exerts a negative feedback effect on glucokinase activity to limit glycogen synthesis in $Cc1^{-/-}$ mice because glycogen energy store is not diminished (4.34 ± 0.61 vs. 2.79 ± 0.56 mg glycogen/g wet tissue in $Cc1^{+/+}$ mice; $P > 0.05$). Although this hypothesis needs to be tested, it supports the notion that increase in G6P content mostly derives from reduced suppressive effect of insulin on gluconeogenesis.

Insulin-stimulated whole-body glucose turnover is unaltered in $Cc1^{-/-}$ mice ($P > 0.05$) (Fig. 2*C*). This is consistent with normal glucose uptake (Fig. 2*F*) and glycolysis (not shown) in skeletal muscle ($P > 0.05$) and with an insignificant decrease in glucose uptake in white adipose tissue ($P > 0.05$) (Fig. 2*H*). Preservation of peripheral insulin sensitivity could compensate for elevation in gluconeogenesis and hepatic insulin resistance and contribute, with decreased G6Pase levels, to lower basal HGP in $Cc1^{-/-}$ (Fig. 2*D*).

Altered lipid metabolism in older inbred $Cc1^{-/-}$ mice. As expected from the positive transcriptional effect of hyperinsulinemia on lipogenic enzymes (23), *Srebp-1c* mRNA (Fig. 3*A*, ii) and FAS protein content (Fig. 4*A*) are elevated in fed 6-month-old $Cc1^{-/-}$ mice. This suggests increased de novo lipogenesis in $Cc1^{-/-}$ mice, as we have previously shown (24). Moreover, fasting serum FFA levels are significantly elevated (~1.5-fold) in parallel to increased visceral adiposity in these mice (Table 1). This suggests increased FFA mobilization out of the adipose tissue and transport into liver, where FFAs are partitioned into the triglyceride synthetic pathways to contribute to increased triglyceride levels beginning at 2 months of age (Table 1).

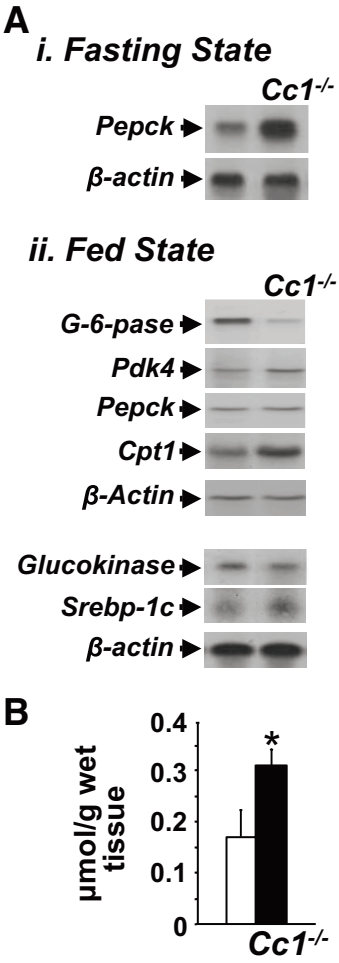

FIG. 3. Northern blot analysis and quantitation of glucose intermediates in livers of inbred mice. Livers from 6-month-old wild-type $Cc1^{+/+}$ (□) and $Cc1^{-/-}$ mice (■) ($n \geq 7$ per group) were isolated for mRNA analysis by Northern blot (*A*) and determination of hepatic G6P levels (*B*). Representative Northern gels from analysis of mRNA levels at fasting and fed states are shown normalized to β-actin. Values expressed as means ± SE. *$P < 0.05$ vs. $Cc1^{+/+}$.

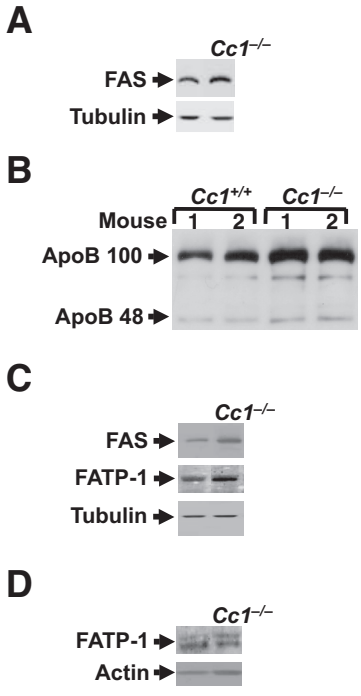

FIG. 4. Western blot analysis of proteins involved in lipid homeostasis in inbred mice. Tissues (*A*, *C*, and *D*) were removed from 6-month-old inbred $Cc1^{-/-}$ mice ($n \geq 5$ per group), and lysates were analyzed by 7% SDS-PAGE and sequential immunoblotting with α-FAS and α-FATP-1 antibodies followed by reprobing with α-tubulin or α-actin antibodies to account for the amount of proteins analyzed. *B*: Serum was diluted and analyzed by 4–10% gradient SDS-PAGE and immunoblotting with an antibody against apolipoprotein (apo)B, which recognizes both apoB48 and apoB100. A representative gel of five to six mice per group is included.

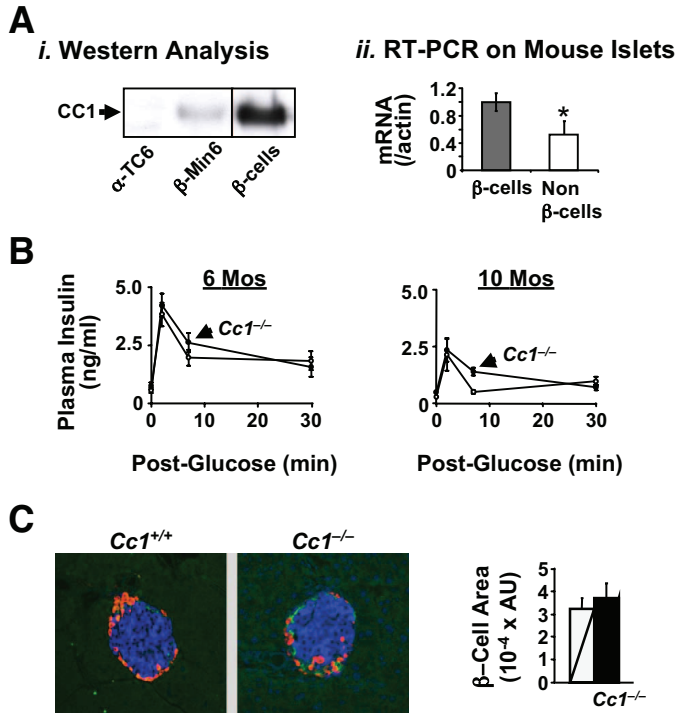

FIG. 5. The effect of Ceacam1 on insulin secretion and β-cell area. *A*: *i*, CEACAM1 protein content in immortalized β-cell islets from βIRKO mice and in α-TC6 and β-Min6 cells was analyzed by Western blot analysis using an antibody against mouse CEACAM1. *ii*, Ceacam1 mRNA levels were determined in FACS-purified β-cells and non–β-cells derived from a normal mouse by real-time PCR analysis. Data are normalized for β-actin and expressed as fold change. *B*: Insulin levels in response to glucose were measured for 0–30 min after intraperitoneal injection of age-matched 6- and 10-month-old inbred *Cc1*$^{+/+}$ (○) and *Cc1*$^{-/-}$ mice (●). Experiments were performed on $n \geq 7$ per group. Values are expressed as means ± SE. *$P < 0.05$ vs. *Cc1*$^{+/+}$. *C*: Pancreas sections from four each of the 6-month-old inbred *Cc1*$^{+/+}$ and *Cc1*$^{-/-}$ mice were fixed and immunostained with antibodies against insulin (blue), glucagon (red), and somatostatin (green). β-Cell area was estimated by morphometric analysis of 44 islets from *Cc1*$^{+/+}$ and 33 from *Cc1*$^{-/-}$ mice. Values expressed as means ± SE in arbitrary units (AU) are presented in the graph. Magnification ×20. (Please see http://dx.doi.org/10.2337/db08-0379 for a high-quality digital representation of this figure.)

Increased hepatic triglyceride content drives increased output, as assessed by elevation in serum ApoB48/ApoB100 protein levels (Fig. 4*B*). With steady-state serum triglyceride levels being normal (Table 1), it is likely that triglyceride is redistributed to the white adipose tissue, as suggested by elevation in FATP-1 and FAS protein content (Fig. 4*C*), rather than to skeletal muscle, in which FATP-1 protein levels are reduced (Fig. 4*D*) and triglyceride content is unaltered (Table 1).

Normal pancreatic β-cell function and area in inbred *Cc1*$^{-/-}$ mice. Western blot analysis reveals that CEACAM1 is highly expressed in FACS-purified mouse pancreatic β-cells (Fig. 5*A*, i). Consistently, CEACAM1 is expressed in murine β-Min6 but not in α-TC6 cells (Fig. 5*A*, i). Quantitative RT-PCR analysis reveals that *Ceacam1* mRNA is expressed at a ratio of ~2:1 in FACS-purified mouse pancreatic β-cells relative to non–β-cells (Fig. 5*A*, ii). Acute-phase insulin secretion in response to glucose remains intact even at 10 months of age, with the area under the curve being comparable with that in *Cc1*$^{+/+}$ mice ($P > 0.05$) (Fig. 5*B*), at which point, both insulin (0.53 ± 0.06 vs. 0.26 ± 0.01 ng/ml in *Cc1*$^{+/+}$ mice; $P < 0.05$) and C-peptide levels (2.73 ± 0.74 vs. 0.39 ± 0.06 ng/ml in *Cc1*$^{+/+}$ mice; $P < 0.05$) are elevated. Moreover, β-cell area is intact in 6-month-old *Cc1*$^{-/-}$ mice, as assessed by immunohistochemical analysis with α-insulin antibody (blue) (Fig. 5*C*). Similarly, immunostaining with α-glucagon (red) reveals normal α-cell area relative to *Cc1*$^{+/+}$ mice. Taken together, the data suggest that Ceacam1 deletion does not adversely affect β-cell area or secretory function.

Earlier onset of insulin resistance in outbred *Cc1*$^{-/-}$ mice. Similar to inbred mice, outbred *Cc1*$^{-/-}$ mice on mixed C57BL/6x129sv background exhibit an increase in body weight and visceral obesity compared with their wild-type counterparts at all ages examined (Table 3).

Outbred *Cc1*$^{-/-}$ mice exhibit hyperinsulinemia (~3- to 4.3-fold) and a ~1.5-fold decrease in insulin clearance beginning at 2 months of age (Table 3). Consistently, glucose level remains suppressed for 3 h after insulin injection in these mice as opposed to *Cc1*$^{+/+}$ mice, in which glucose levels return to basal within 2 h (Fig. 6*A*). Impaired insulin clearance yields insulin resistance starting at 2 months of age, as indicated by random hyperglycemia (Table 3) and glucose intolerance (Fig. 6*B*; with blood glucose of 387 ± 92 vs. 185 ± 18 mg/dl in *Cc1*$^{+/+}$ mice at 2 h after glucose injection; $P < 0.0001$). Because glucose levels decrease to a similar extent in 2- (Fig. 6*A*) and 6-month-old outbred *Cc1*$^{-/-}$ and *Cc1*$^{+/+}$ mice after insulin injection (not shown), insulin response in peripheral tissues appears to be normal. Western blot analysis of immunopellets of the insulin receptor β-subunit (IR_β) using phosphotyrosine antibody (α-pTyr), reveals decreased ability of insulin to induce IR_β phosphorylation in liver lysates of 2-month-old *Cc1*$^{-/-}$ compared with *Cc1*$^{+/+}$ mice (Fig. 6*C*). Outbred *Cc1*$^{-/-}$

TABLE 3
Metabolic parameters of outbred B6x129sv mice

	2 months		6 months	
	Cc1$^{+/+}$	*Cc1*$^{-/-}$	*Cc1*$^{+/+}$	*Cc1*$^{-/-}$
Body wt (g)	23.7 ± 0.85	26.9 ± 0.92*	31.0 ± 1.10	35.2 ± 0.84*
% Visceral fat/body wt	1.22 ± 0.10	2.00 ± 0.13*	1.81 ± 0.27	3.37 ± 0.35*
Serum insulin (ng/ml)	0.51 ± 0.09	1.57 ± 0.29*	0.25 ± 0.03	1.04 ± 0.26*
Serum C-peptide (ng/ml)	2.69 ± 0.36	5.34 ± 0.93*	2.04 ± 0.14	3.28 ± 0.56*
Steady-state C/I	5.89 ± 0.85	3.50 ± 0.66*	4.42 ± 0.28	3.39 ± 0.31*
Serum FFA (mEq/l)	0.40 ± 0.02	0.75 ± 0.09*	0.50 ± 0.04	1.12 ± 0.15*
Serum triglyceride (mg/dl)	53.3 ± 5.20	78.2 ± 7.80*	59.6 ± 5.25	84.9 ± 8.41*
Fasting glucose (mg/dl)	96.2 ± 3.62	96.5 ± 3.40	81.3 ± 1.10	87.9 ± 6.64
Random glucose (mg/dl)	134. ± 5.22	151. ± 5.40*	133. ± 9.90	157. ± 9.54*

Data are means ± SE. *$P < 0.05$ Cc1$^{-/-}$ vs. *Cc1*$^{+/+}$ control mice.

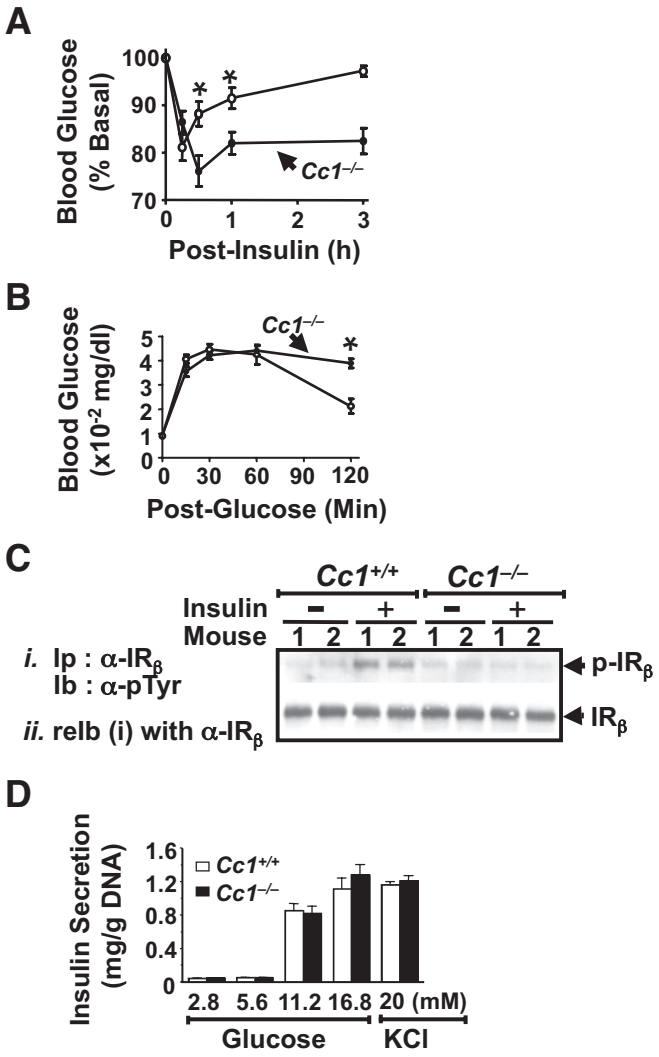

FIG. 6. Insulin resistance in outbred C57BL/6x129sv mice. *A*: For insulin tolerance, glucose levels were measured in venous blood extracted from overnight-fasted 6-month-old age-matched wild-type $Cc1^{+/+}$ (○) and $Cc1^{-/-}$ mice (●) injected intraperitoneally with 0.125 units/kg insulin for 0–3 h. Experiments were performed on $n \geq 9$ per group. Values are expressed as means ± SE. *$P < 0.05$ vs. $Cc1^{+/+}$. *B*: For glucose tolerance test, blood glucose level was determined in overnight-fasted 2-month-old $Cc1^{+/+}$ (○) and $Cc1^{-/-}$ mice (●) mice at 0–120 min after intraperitoneal glucose injection (2 g/kg). Six to 11 mice were used in each group. Values are expressed as means ± SE. *$P < 0.05$ vs. $Cc1^{+/+}$. *C*: For Western blot analysis of insulin receptor phosphorylation, liver lysates of 2-month-old outbred $Cc1^{-/-}$ and $Cc1^{+/+}$ controls were incubated with (+) or without (−) 100 nmol/l insulin. The IR_β was immunoprecipitated (Ip), analyzed by 7% SDS-PAGE, and transferred to nitrocellulose membrane for immunoblotting (Ib) with horseradish peroxidase–conjugated phosphotyrosine (α-pTyr) antibody (*i*). Membranes were reprobed (reIb) with α-IR_β antibody to account for the amount of insulin receptor in the immunopellets (*ii*). The gel is representative of three different experiments each performed on two mice per treatment per group. *D*: Islets were isolated from 6-month-old wild-type $Cc1^{+/+}$ (□) and $Cc1^{-/-}$ mice (■) ($n > 3$ per group) by collagenase digestion followed by centrifugation over histopaque gradient. Recovered islets were cultured overnight in RPMI containing 5.5 nmol/l glucose. Insulin secretion was assayed by incubating 10 islets in Kreb's buffer containing different concentrations of glucose or 20 mmol/l KCl for 1 h. Amount of insulin secreted was normalized with DNA content, and values are expressed as means ± SE.

mice also exhibit elevation in fasting serum FFA and triglyceride levels starting at 2 months of age (Table 3). Taken together, the data suggest that outbred $Cc1^{-/-}$ mice develop altered lipid metabolism and insulin resistance, primarily in liver, with a more rapid onset than the inbred mice.

Serum C-peptide levels are mildly elevated (by ~1.5-fold) in outbred $Cc1^{-/-}$ mice (Table 3), suggesting compensatory increase in insulin secretion. Acute-phase insulin secretion in response to glucose is intact (not shown), and insulin secretion in response to increasing glucose levels and 20 mmol/l KCl is normal in primary islets derived from 6-month-old outbred $Cc1^{-/-}$ mice (Fig. 6*D*). Fasting serum glucagon level is also normal in these mice (40.19 ± 0.89 vs. 42.36 ± 1.99 pg/ml in $Cc1^{+/+}$ mice; $P > 0.05$). This suggests that Ceacam1 deletion does not affect insulin secretion when propagated on the mixed C57BL/6x129sv background.

DISCUSSION

L-SACC1 transgenic mice with liver inactivation of CEACAM1 demonstrated that CEACAM1 promotes insulin action by coordinated regulation of insulin and lipid metabolism (8,10,24). The purpose of this study was to use the null $Cc1^{-/-}$ mouse to reevaluate the role of CEACAM1 in insulin action in the absence of the potential confounding effect of the dominant-negative transgene. We herein report that homozygosity for a null Cc1 allele phenocopies transgenic inactivation of CEACAM1 in liver and causes visceral obesity together with impairment of insulin clearance and hyperinsulinemia, followed by insulin resistance, with an earlier onset when propagated on a mixed C57BL/6x129sv relative to pure C57BL/6 background (as with null mutation of the insulin receptor substrate 2 gene [25,26]). Despite abundant expression in β-cells, null mutation of Ceacam1 does not reduce β-cell secretory function or β-cell area in response to glucose. This supports a key role for CEACAM1 in promoting hepatic insulin clearance.

Like its liver-specific inactivation, null mutation of Ceacam1 impairs insulin clearance and causes hyperinsulinemia and hepatic insulin resistance in association with increased steatosis. These findings are consistent with the high expression of CEACAM1 in liver (27), a major site for insulin clearance. We have shown that CEACAM1-dependent pathways mediate a decrease in FAS activity to protect the liver from the lipogenic effect of high insulin levels in portal vein and that this effect is abolished in the hyperinsulinemic Ceacam1 mutant mice (24). Together with increased *Srebp-1c* mRNA and FAS protein levels, this leads to increased de novo lipogenesis and contributes to increase in hepatic triglyceride content in $Cc1^{-/-}$ mice. Moreover, these mice exhibit a reduction in the suppressive effect of insulin on lipid oxidation and gluconeogenesis, which is manifested by increased G6P content, which, in association with reduced *G6Pase* mRNA level (and presumably activity), is partitioned to the triglyceride synthetic pathways. The data suggest that null mutation of Ceacam1 chronically gears the liver toward steatosis by increasing hepatic FFA supply and de novo lipogenesis in addition to increasing G6P production and its partitioning toward triglyceride synthesis.

Consistent with a positive correlation between liver steatosis, hyperinsulinemia, and high serum ApoB levels in humans and rodents (23,28–31), serum ApoB100/48 levels are elevated in $Cc1^{-/-}$ mice, suggesting increased triglyceride output. Normal circulating triglyceride levels support redistribution into peripheral tissues in response to compensatory increase in insulin secretion. As in leptin deficiency (32) and transgenic lipoatrophic AZIP mutation (33), propagation of Ceacam1 deletion on the C57BL/6 genetic background favors substrate redistribution to the

adipose tissue rather than muscle. Although this leads to visceral obesity in *Cc1*$^{-/-}$ mice, it does not adversely affect insulin action in the periphery, in particular in muscle, where fatty acid uptake is reduced and triglyceride content is normal. Selective increase in triglyceride accumulation and alteration of insulin action in liver as opposed to muscle appears to be common in the C57BL/6 strain, as has been suggested by the phenotype of *Ob/Ob* (32) and lipoatrophic AZIP mice (33), which when propagated onto the FVB background exhibit triglyceride partitioning from liver to muscle. Likewise, transgenic inactivation of CEACAM1 in liver causes insulin resistance and fat accumulation in muscle and adipose tissue, in addition to liver, when propagated on a C57BL/6xFVB mixed background (8). In light of the modulation of the diabetes phenotype by strain-related genetic factors (34), it is possible that Ceacam1-null mutation would cause insulin resistance in muscle if propagated on the FVB genetic background. Conditional null mutation of the insulin receptor in liver yields hepatic insulin resistance with elevated lipogenesis and serum ApoB100/48 but with reduced serum triglycerides in comparison with wild-type mice (35). Whereas this mouse emphasizes the impact of interrupted insulin signaling at the receptor level on steatosis in liver, the *Cc1*$^{-/-}$ mouse phenotype highlights the critical role of CEACAM1 in regulating insulin action by coordinating insulin and lipid metabolism in liver and subsequently in extrahepatic tissues. This in vivo demonstration of a distinct CEACAM1-dependent postreceptor signaling pathway modulating insulin action by promoting insulin clearance provides proof of principle that hyperinsulinemia and hepatic steatosis can be a primary cause of insulin resistance, rather than a marker thereof.

Null mutation of Ceacam1 alters neither the insulin secretory function of β-cells in response to glucose nor β-cell area. Because β-cell–specific null mutation of insulin receptor (βIRKO) causes reduction in acute-phase insulin secretion in response to glucose (18), our finding suggests that CEACAM1 does not modulate the insulin signaling pathways mediating insulin secretion. It remains possible that deletion of Ceacam1 is compensated for by Ceacam2, a close relative of Ceacam1 (36), whose expression, albeit lower than that of Ceacam1 in β-cells, is not significantly altered in the *Cc1*$^{-/-}$ mouse (not shown).

Taken together, the data suggest that the primary metabolic effect of *Cc1* deficiency is impaired insulin clearance rather than increased insulin secretion. The underlying mechanism of insulin resistance induced by hyperinsulinemia is a manifestation of several metabolic and cellular abnormalities, including increased lipogenesis in liver. This paradigm assigns a primary role for CEACAM1 in regulating insulin action by promoting insulin clearance and regulating lipogenesis in liver.

ACKNOWLEDGMENTS

R.N.K. has received National Institutes of Health Grant DK-67536. J.K.K. has received grants from the American Diabetes Association and the Pennsylvania State Department of Health. S.M.N. has received National Institutes of Health Grant DK-54254, a grant from the American Diabetes Association, and U.S. Department of Agriculture Grant USDA 38903-02315.

We thank Dr. N. Beauchemin (McGill University, Montreal, Canada) for providing the mice. We also thank Drs. Jill Schroeder-Gloeckler and Qusai Y. Al-Share and Mats Fernstrom for technical assistance and scientific discussions.

REFERENCES

1. Duckworth WC, Bennett RG, Hamel FG: Insulin degradation: progress and potential. *Endocrinol Rev* 19:608–624, 1998
2. Shillabeer G, Hornford J, Forden JM, Wong NC, Russell JC, Lau DC: Fatty acid synthase and adipsin mRNA levels in obese and lean JCR:LA-cp rats: effect of diet. *J Lipid Res* 33:31–39, 1992
3. Assimacopoulos-Jeannet F, Brichard S, Rencurel F, Cusin I, Jeanrenaud B: In vivo effects of hyperinsulinemia on lipogenic enzymes and glucose transporter expression in rat liver and adipose tissues. *Metabolism* 44:228–233, 1995
4. Rabkin R, Ryan MP, Duckworth WC: The renal metabollism of insulin. *Diabetologia* 27:351–357, 1984
5. Formisano P, Najjar SM, Gross CN, Philippe N, Oriente F, Kern BCL, Accili D, Gorden P: Receptor-mediated internalization of insulin: potential role of pp120/HA4, a substrate of the insulin receptor kinase. *J Biol Chem* 270:24073–24077, 1995
6. Li Calzi S, Choice CV, Najjar SM: Differential effect of pp120 on insulin endocytosis by two variant insulin receptor isoforms. *Am J Physiol* 273:E801–E808, 1997
7. Najjar SM, Choice CV, Soni P, Whitman CM, Poy MN: Effect of pp120 on receptor-mediated insulin endocytosis is regulated by the juxtamembrane domain of the insulin receptor. *J Biol Chem* 273:12923–12928, 1998
8. Poy MN, Yang Y, Rezaei K, Fernström MA, Lee AD, Kido Y, Erickson SK, Najjar SM: CEACAM1 regulates insulin clearance in liver. *Nat Genet* 30:270–276, 2002
9. Dubois MJ, Bergeron S, Kim HJ, Dombrowski L, Perreault M, Fournes B, Faure R, Olivier M, Beauchemin N, Shulman GI, Siminovitch KA, Kim JK, Marette A: The SHP-1 protein tyrosine phosphatase negatively modulates glucose homeostasis. *Nat Med* 12:549–556, 2006
10. Park SY, Cho YR, Kim HJ, Hong EG, Higashimori T, Lee SJ, Goldberg IJ, Shulman GI, Najjar SM, Kim JK: Mechanism of glucose intolerance in mice with dominant negative mutation of CEACAM1. *Am J Physiol Endocrinol Metab* 291:E517–E524, 2006
11. Leung N, Turbide C, Olson M, Marcus V, Jothy S, Beauchemin N: Deletion of the carcinoembryonic antigen-related cell adhesion molecule 1 (Ceacam1) gene contributes to colon tumor progression in a murine model of carcinogenesis. *Oncogene* 25:5527–5536, 2006
12. Dai T, Abou-Rjaily GA, Al-Share' QY, Yang Y, Fernström MA, DeAngelis AM, Lee AD, Sweetman L, Amato A, Pasquali M, Lopaschuk GD, Erickson SK, Najjar SM: Interaction between altered insulin and lipid metabolism in CEACAM1-inactive transgenic mice. *J Biol Chem* 279:45155–45161, 2004
13. Powers AC, Efrat S, Mojsov S, Spector D, Habener JF, Hanahan D: Proglucagon processing similar to normal islets in pancreatic α-like cell line derived from transgenic mouse tumor. *Diabetes* 39:406–414, 1990
14. Miyazaki J, Araki K, Yamato E, Ikegami H, Asano T, Shibasaki Y, Oka Y, Yamamura K: Establishment of a pancreatic beta cell line that retains glucose-inducible insulin secretion: special reference to expression of glucose transporter isoforms. *Endocrinology* 127:126–132, 1990
15. Najjar SM, Philippe N, Suzuki Y, Ignacio GA, Formisano P, Accili D, Taylor SI: Insulin-stimulated phosphorylation of recombinant pp120/HA4, an endogenous substrate of the insulin receptor tyrosine kinase. *Biochemistry* 34:9341–9349, 1995
16. Sadekova S, Lamarche-Vane N, Li X, Beauchemin N: The CEACAM1-L glycoprotein associates with the actin cytoskeleton and localizes to cell-cell contact through activation of Rho-like GTPases. *Mol Biol Cell* 11:65–77, 2000
17. Kitamura T, Kido Y, Nef S, Merenmies J, Parada LF, Accili D: Preserved pancreatic beta cell function in mice lacking the insulin receptor-related receptor. *Mol Cell Biol* 21:5624–5630, 2001
18. Kulkarni RN, Bruning JC, Winnay JN, Postic C, Magnuson MA, Kahn CR: Tissue-specific knockout of the insulin receptor in pancreatic beta cells creates an insulin secretory defect similar to that in type 2 diabetes. *Cell* 96:329–339, 1999
19. Josefsen K, Stenvang JP, Kindmark H, Berggren PO, Horn T, Kjaer T, Buschard K: Fluorescence-activated cell sorted rat islet cells and studies of the insulin secretory process. *J Endocrinol* 149:145–154, 1996
20. Morioka T, Asilmaz E, Hu J, Dishinger JF, Kurpad AJ, Elias CF, Li H, Elmquist JK, Kennedy RT, Kulkarni RN: Disruption of leptin receptor expression in the pancreas directly affects beta cell growth and function in mice. *J Clin Invest* 117:2860–2868, 2007
21. DeFronzo RA: Lilly lecture 1987. The triumvirate: β-cell, muscle, liver. A collusion responsible for NIDDM. *Diabetes* 37:667–687, 1988

22. Chen X, Iqbal N, Boden G: The effects of free fatty acids on gluconeogenesis and glycogenolysis in normal subjects. *J Clin Invest* 103:365–372, 1999
23. Horton JD, Goldstein JL, Brown MS: SREBPs: activators of the complete program of cholesterol and fatty acid synthesis in the liver. *J Clin Invest* 109:1125–1131, 2002
24. Najjar SM, Yang Y, Fernstrom MA, Lee SJ, Deangelis AM, Rjaily GA, Al-Share QY, Dai T, Miller TA, Ratnam S, Ruch RJ, Smith S, Lin SH, Beauchemin N, Oyarce AM: Insulin acutely decreases hepatic fatty acid synthase activity. *Cell Metab* 2:43–53, 2005
25. Kushner JA, Ye J, Schubert M, Burks DJ, Dow MA, Flint CL, Dutta S, Wright CV, Montminy MR, White MF: Pdx1 restores beta cell function in Irs2 knockout mice. *J Clin Invest* 109:1193–1201, 2002
26. Suzuki R, Tobe K, Terauchi Y, Komeda K, Kubota N, Eto K, Yamauchi T, Azuma K, Kaneto H, Taguchi T, Koga T, German MS, Watada H, Kawamori R, Wright CV, Kajimoto Y, Kimura S, Nagai R, Kadowaki T: Pdx1 expression in Irs2-deficient mouse beta-cells is regulated in a strain-dependent manner. *J Biol Chem* 278:43691–43698, 2003
27. Accili D, Perrotti N, Rees JR, Taylor SI: Tissue distribution and subcellular localization of an endogenous substrate (pp120) for the insulin receptor-associated tyrosine kinase. *Endocrinology* 119:1274–1280, 1986
28. Elam MB, Wilcox HG, Cagen LM, Deng X, Raghow R, Kumar P, Heimberg M, Russell JC: Increased hepatic VLDL secretion, lipogenesis, and SREBP-1 expression in the corpulent JCR:LA-cp rat. *J Lipid Res* 42:2039–2048, 2001
29. Ginsberg HN, Zhang YL, Hernandez-Ono A: Regulation of plasma triglycerides in insulin resistance and diabetes. *Arch Med Res* 36:232–240, 2005
30. Matikainen N, Manttari S, Westerbacka J, Vehkavaara S, Lundbom N, Yki-Jarvinen H, Taskinen MR: Postprandial lipemia associates with liver fat content. *J Clin Endocrinol Metab* 92:3052–3059, 2007
31. Vine DF, Takechi R, Russell JC, Proctor SD: Impaired postprandial apolipoprotein-B48 metabolism in the obese, insulin-resistant JCR:LA-cp rat: increased atherogenicity for the metabolic syndrome. *Atherosclerosis* 190:282–290, 2007
32. Haluzik M, Colombo C, Gavrilova O, Chua S, Wolf N, Chen M, Stannard B, Dietz KR, Le Roith D, Reitman ML: Genetic background (C57BL/6J versus FVB/N) strongly influences the severity of diabetes and insulin resistance in ob/ob mice. *Endocrinology* 145:3258–3264, 2004
33. Colombo C, Haluzik M, Cutson JJ, Dietz KR, Marcus-Samuels B, Vinson C, Gavrilova O, Reitman ML: Opposite effects of background genotype on muscle and liver insulin sensitivity of lipoatrophic mice: role of triglyceride clearance. *J Biol Chem* 278:3992–3999, 2003
34. Clee SM, Attie AD: The genetic landscape of type 2 diabetes in mice. *Endocr Rev* 28:48–83, 2007
35. Biddinger SB, Hernandez-Ono A, Rask-Madsen C, Haas JT, Aleman JO, Suzuki R, Scapa EF, Agarwal C, Carey MC, Stephanopoulos G, Cohen DE, King GL, Ginsberg HN, Kahn CR: Hepatic insulin resistance is sufficient to produce dyslipidemia and susceptibility to atherosclerosis. *Cell Metab* 7:125–134, 2008
36. Han E, Phan D, Lo P, Poy MN, Behringer R, Najjar SM, Lin S-H: Differences in tissue-specific and embryonic expression of mouse Ceacam1 and Ceacam2 genes. *Biochem J* 355:417–423, 2001